Received September 1999
Revised March 2000
Accepted May 2000

Enhancing forced convection by inserting porous substrate in the core of a parallel-plate channel

M.O. Hamdan, M.A. Al-Nimr and M.K. Alkam
Mechanical Engineering Department, Jordan University of Science and Technology, Irbid, Jordan

Keywords *Forced convection, Porous media*

Abstract *Investigates numerically the mechanism of enhancing heat transfer by using porous substrate. The numerical investigation is carried out for transient forced convection in the developing region of a parallel-plate channel partially filled with a porous medium. A porous substrate is inserted in the channel core in order to reduce the boundary layer thickness and hence, enhance heat transfer. Darcy-Brinkman-Forchheimer model is used to simulate the physical problem. Results of the current model show that the existence of the porous substrate may improve the Nusselt number at the fully developed region by a factor of four and even higher depending on the value of Darcy number. It is found that the maximum Nusselt number is achieved at an optimum thickness. Also, the study shows that partially filled channels have better thermal performance than the totally filled ones. However, there is an optimum thickness of porous substrate, beyond it the Nusselt number starts to decline.*

Nomenclature

A = microscopic inertial coefficient or form drag coefficient, $\frac{\varepsilon F \ell}{\rho_R \sqrt{K}}$
C = specific heat constant
Da = Darcy number, K/ℓ^2
e = dimensionless porous substrate thickness, $\frac{\ell_2 - \ell_1}{\ell} = \frac{L_2 - L_1}{L}$
F = Forchheimer coefficient, $\frac{1.8}{(180\varepsilon^5)^{0.5}}$
K = permeability of the porous substrate
k_1 = thermal conductivity of the fluid
k_2 = thermal conductivity of porous domain, $k_f\varepsilon + k_s(1 - \varepsilon)$
k_R = thermal conductivity ratio, k_2/k_1
L = dimensionless duct height, $\ell/\ell = 1$
Nu = local Nusselt number, $2h\ell/k_1$
P = dimensionless pressure, $p\ell^2/\rho_1 \nu^2_1$
p = pressure
Pr = Prandtl number of the fluid, $C_1 \mu_1/k_1$
Q = dimensionless accumulated heat transfer conducted from walls, $\int_0^{X_d} \frac{k_w}{T_w - T_o} \frac{\partial \theta}{\partial Y} dX$
T = temperature at any point
T_m = mixing cup temperatures over any cross-section, MCT. $= \frac{\int_0^{l_1} C_1\rho_1 u_1 T_1 dy + \int_{l_1}^{l_2} C_2\rho_2 u_1 T_2 dy + \int_{l_1}^{1} C_1\rho_1 u_1 T_1 dy}{\rho_o u_o \ell}$
T_o = initial temperature
T_w = temperature of the isothermal wall
t = time
u = axial velocity
u_o = inlet axial velocity
U = dimensionless volume averaged axial velocity, $u\ell/v_1$
U_o = dimensionless inlet axial velocity, $u_o\ell/v_1$
v = transverse velocity
V = dimensionless transverse velocity, $v\ell/v_1$
x = dimensional axial coordinate
X = dimensionless axial coordinate, $\frac{x}{\ell}$
X_d = axial distance that is longer than hydrodynamic entrance length

International Journal of Numerical Methods for Heat & Fluid Flow, Vol. 10 No. 5, 2000, pp. 502-517.

y = dimensional transverse coordinate
Y = dimensionless transverse coordinate, $\frac{y}{\ell}$

Greek symbols
ρ = density
θ = dimensionless temperature, $(T - T_i)/(T_o - T_i)$
θ_m = dimensionless mixing cup temperature $(T_m - T_i)/(T_o - T_i)$
τ = dimensionless time, $t\ v/\ell^2$
μ = dynamic viscosity
σ = heat capacity ratio, $\left[\rho_f C_{pf}\varepsilon + \rho_2 C_s(1-\varepsilon)\right]/\varepsilon\rho_f C_{pf}$
Δ = increment in numerical mesh network space
ν = kinematic viscosity
ε = porosity
ν_R = kinematic viscosity ratio, ν_2/ν_1

Subscripts
0 = inlet properties
1 or f = fluid domain properties
2 or p = effective porous domain properties
R = the ratio of a parameter in porous domain to the same parameter in fluid domain
s = solid matrix properties
w = wall conditions

Introduction

Enhancing heat transfer by porous media is an area of interest for several researches. The mechanism of enhancing heat transfer by using porous media is referred to: reducing boundary layer thickness; using high thermal conductive porous media; and increasing the effective area of heat transfer. The porous insertion is countered in many engineering applications due to its high performance. Therefore, several numerical and experimental studies have been conducted in order to provide a deeper understanding of the transport mechanism of momentum and heat transfer in porous media. Porous media have a wide range of applications such as catalytic and inert packed bed reactors, enhancing drying efficiency such as food drying, filtering, geothermal energy management and harvesting, insulation, lubrication (Kaviany, 1995), laser mirrors and powerful electronics (Jiang *et al.*, 1996), ground water and oil flow, and enhancing oil and natural gas production. High thermal conductivity porous substrates are also used to enhance forced convection heat transfer in many engineering applications such as, nuclear cooling, heat exchangers, and solar collectors (Alkam and Al-Nimr, 1999a).

Recently, heat transfer in channels partially filled with a porous media has received considerable attention and was the focus of several investigations (Al-Nimr and Alkam, 1997; Chikh *et al.*, 1995a; Vafai and Kim, 1990; Poulikakos and Kazierczak, 1987). As previously mentioned, the need for better understanding of heat transfer in porous media is motivated by the numerous engineering applications encountered.

In general, most analytical studies of fluid flow and heat transfer adopt Darcy's law. Carman (1956) and Collins (1961) have investigated the fluid flow through porous material using Darcy's law. In recent research conducted by Al-Nimr and Alkam (1998) and Alkam *et al.* (1998), there appears to be very limited research on the problem of forced convection in composite fluid and porous layers. Beavers and Joseph (1967) first investigated the fluid mechanics at the interface between a fluid layer and a porous medium over a flat plate. Vafai and Thiyagaraja (1987) obtained an analytical approximate solution for

the same problem based on matched asymptotic expansions for the velocity and temperature distributions. Later on, Vafai and Kim (1995) presented an exact solution for the same problem. Closed form analytical solutions for forced convection in parallel plate ducts and in circular pipes partially filled with porous materials were obtained by Poulikakos and Kazierczak (1987) for constant wall heat flux. The same previous group presented numerical results computed for constant wall temperature but for completely filled ducts (Poulitakos and Renken, 1987). Using Darcy-Brinkman-Forchheimer model, the problem of forced convection in channels partially filled with porous media was numerically investigated by Jang and Chen (1992). Rudraiah (1985) investigated the same problem using the Darcy-Brinkman model. Also, using the Darcy-Brinkman model, analytical solutions were obtained by Chikh *et al.* (1995a) for the problem of forced convection in an annular duct partially filled with a porous medium. In Chikh *et al.* (1995b), the same problem was investigated numerically by the same group using the Darcy-Brinkman-Forchheimer model. Chen and Vafai (1996) investigated free surface momentum and heat transfer in porous domain using a finite difference scheme. Nield (1991) discussed the limitation of the Brinkman-Forchheimer model in porous media and at the interface, between the clear fluid and porous region.

The transient response of circular and annular channels partially filled with porous materials under forced convection conditions was investigated numerically by Alkam and Al-Nimr (1998), and Al-Nimr and Alkam (1997), respectively. The same two authors have used porous substrates to improve the thermal performance of solar collectors (Alkam and Al-Nimr, 1999a), and heat exchanger (Alkam and Al-Nimr, 1999b). Also, they have investigated the transient behavior of a channel partially filled with porous substrate from hydrodynamic point of view (Al-Nimr and Alkam, 1998).

This study shows the benefits of using porous substrate rather than filling the entire duct with porous media. This investigation considers the problem of transient forced convection flow in parallel-plate channels partially filled with porous substrate inserted in the channel core using Brinkman-Forchheimer model. The effect of different operating and flow parameters on the thermal performance of the channel will be investigated. These parameters include the porous substrate thickness, the thermal conductivity of the porous substrate, the microscopic inertial coefficient, and the Darcy number.

Problem formulation

Figure 1 represents the investigated problem scheme with its coordinate system. The scheme considers two-dimensional flow through two isothermal parallel-plate channels partially filled with porous substrate inserted in the core of the channel. The transient thermal state is maintained by imposing a sudden change on the wall temperature. The steady state flow enters the channel with a uniform velocity distribution, u_o, and constant temperature, T_o. Initially, the fluid and the wall have the same temperature. Forchheimer-Brinkman Darcy

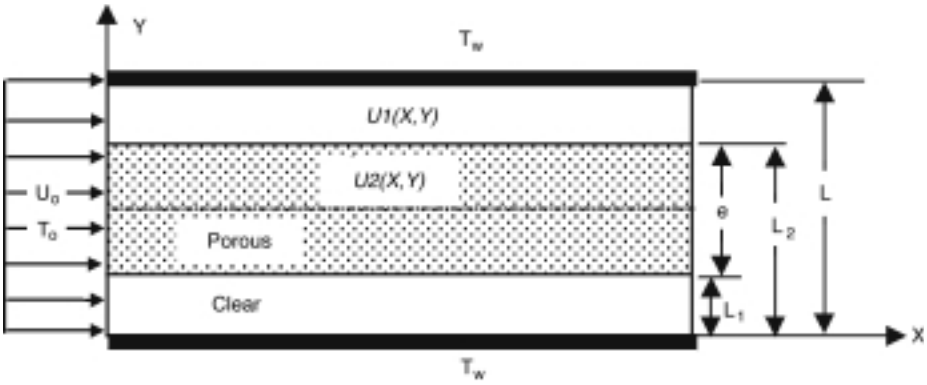

Figure 1.
A schematic diagram of the problem under consideration

model is adopted assuming laminar, single phase, boundary layer flow with no internal heat generation, and neglecting viscous dissipation and axial conduction. Also, it is assumed that the porous medium is homogeneous, isotropic, consolidated, saturated with fluid, with invariant thermal properties, and chemically stable. The fluid is homogeneous, incompressible and in local thermal equilibrium with the solid matrix.

From continuum viewpoint, porous-medium and clear-fluid domains can be treated as one domain by properly accounting for the role of each domain. Therefore, and due to the corresponding of conservation equation in porous medium and clear-fluid domains, the interface condition is eliminated. Using the dimensionless parameter given in the nomenclature based on the viscous velocity scale, the equations of continuity, momentum, and energy equation, for both clear and porous domains, reduce to the following dimensionless equations:

$$\frac{\partial \mathrm{U}}{\partial \mathrm{X}} + \frac{\partial \mathrm{V}}{\partial \mathrm{Y}} = 0 \tag{1}$$

$$\mathrm{U}\frac{\partial \mathrm{U}}{\partial \mathrm{X}} + \mathrm{V}\frac{\partial \mathrm{U}}{\partial \mathrm{Y}} = -[\lambda(\frac{1}{\rho_{\mathrm{R}}} - 1) + 1]\frac{\partial \mathrm{P}}{\partial \mathrm{X}} + [\lambda(\nu_{\mathrm{R}} - 1) + 1] \frac{\partial^2 \mathrm{U}}{\partial \mathrm{Y}^2} - \lambda[\frac{\nu_{\mathrm{R}}}{\mathrm{Da}}\mathrm{U} + \mathrm{AU}^2] \tag{2}$$

$$\frac{\partial \theta}{\partial \tau} + \mathrm{U}\frac{\partial \theta}{\partial \mathrm{X}} + \mathrm{V}\frac{\partial \theta}{\partial \mathrm{Y}} = [\lambda(\frac{\mathrm{k_R}}{\mathrm{Pr_1}} - 1) + 1]\frac{\partial^2 \theta}{\partial \mathrm{Y}^2} \tag{3}$$

Where λ is a binary parameter, the values of which are zero in the clear layer and 1.0 in the porous layer. It is important to mention that the value of effective viscosity ratio μ_{R} is not settled. However, the value of $\mu_{\mathrm{R}} = 1$ has been used successfully in several studies exemplified by Poulikakos and Kazierczak (1987) and Chikh *et al.* (1995a). In fact, $\mu_{\mathrm{R}} = 1$ is a good approximation in the

range of $0.7 < \varepsilon < 1$. It is noticeable that the transverse momentum equation has been eliminated due to the boundary layer simplification. Referring to Bodoia and Ostrele (1961) and due to the lack of transverse momentum equation, the integral form of continuity equation is used to compensate for such equation.

$$\int_0^{L_1} U_1 dY + \int_{L_1}^{L_2} \rho_R U_2 dY + \int_{L_2}^{L} U_1 dY = U_0 L \tag{4}$$

The conditions required for the momentum equation are boundary conditions, and at the walls and at the inlet of the duct.

$$\begin{array}{lll} \text{at} & X = 0 \text{ and} & 0 < Y < L \\ & & U_1 = U_2 = U_o \text{ and } V_1 = V_2 = V_o \\ \text{for} & X > 0 \text{ and} & Y = 0 \\ & & U_1 = V_1 = 0 \\ \text{for} & X > 0 \text{ and} & Y = L \\ & & U_1 = V_1 = 0 \end{array} \tag{5}$$

The energy equation has the following initial conditions:

$$\text{at } \tau = 0 \qquad \theta_1 = \theta_2 = 0 \tag{6}$$

for $\tau > 0$, the thermal boundary, at the walls and at the inlet of the duct, and interface conditions are:

$$\begin{array}{lll} \text{at} & X = 0 \text{ and} & 0 < Y < L \\ & & \theta_1 = \theta_2 = 0 \\ \text{for} & X > 0 \text{ and} & Y = 0 \\ & & \theta_1 = 1 \\ \text{for} & X > 0 \text{ and} & Y = L \\ & & \theta_1 = 1 \end{array} \tag{7}$$

Interface condition was not used due to using the continuum viewpoint.

The local Nusselt number and mixing cup temperature is defined as follow:

$$Nu = \frac{2h\ell}{k_f} = \frac{2}{1 - \theta_m} \left.\frac{\partial \theta}{\partial Y}\right|_{Y=0}, \qquad \text{where} \qquad \theta_m = \frac{T_m - T_o}{T_w - T_o}$$

Numerical solution

Implicit finite difference technique was used to simulate the problem under consideration. Therefore, a three-dimensional mesh was imposed on the solution domain to resemble the independent variables X, Y and τ. The non-dimensional time, τ, is simulated as a third coordinate, normal to the X-Y plane.

The non-linear terms in momentum equation were linearized by using the lagging technique (Hoffman, 1992). The linearized implicit finite difference equations are derived using second-order central difference scheme for the transverse derivatives, and first-order backward scheme for both the axial and time derivatives. The consistency and stability of the discretized governing equations have been checked, and it is found that the derived forms are consistent and unconditionally stable for the time domain.

Numerical methods that discussed by Bodoia and Osterle (1961) and El-Shaarawi and Alkam (1992) are used to solve the finite difference equations that simulate the flow hydrodynamics at steady state conditions. The linearized momentum finite difference equation, together with boundary conditions, is transformed to a set of algebraic equations. This set of equations was solved by using Gauss-Jordan elimination method (Hoffman, 1992). Having obtained the values of U_1, U_2, V_1 and V_2 over the flow field, the discretized energy equations are solved by marching in time. The finite difference energy equation is transformed to tridiagonal set of algebraic equations that are solved by Thomas algorithm (Hoffman, 1992). The solution procedure in time is carried out until steady-state conditions are practically achieved.

In order to perform the grid refinement test, several runs were performed and the optimum step sizes in X and Y directions are reported on Table I. This solution gained is independent of the time grid size. The optimization of the grid size based on computing of the local Nusselt number at an arbitrary axial location, employing a given number of grid points in both the transverse and axial directions. After that the number of grid points is increased gradually, and each time, a computer run is performed to compute the local Nusselt number. The procedure is continued until variation of the local Nusselt number

	ΔX [m]					
ΔY [n]	0.05 [4]	0.01 [10]	0.005 [20]	0.001 [100]	0.0005 [200]	0.0001 [1,000]
0.02 [50]	69.7308	26.5214	23.4415	21.6234	21.439	21.3013
0.0143 [70]	74.1657	26.6461	23.6514	21.9432	21.7841	21.6680
0.01 [100]	77.0754	26.7589	23.8079	22.1618	22.0257	21.9342
0.0083 [120]	78.0453	26.8141	23.8714	22.2394	22.1126	22.0333
0.0067 [150]	78.8954	26.8755	23.9367	22.3118	22.1935	22.2666
0.0056 [180]	79.3848	26.9191	23.9809	22.3570	22.2432	22.2229
0.005 [200]	79.6037	26.9415	24.0029	22.3787	22.2666	22.2163

Note: n: number of grids on Y-direction; m: number of grids on X-direction

Table I.
Grid refinement depending on Nusselt number: U = 100, at X = 0.1, and L_2 = L 20 per cent porous substrate thickness

fixed for the first digit. At this point the spatial grid size is fixed. The optimum choice is $\Delta X = 10^{-4}$, $\Delta Y = 0.005$ and $\Delta\tau = 0.001$, as shown in Table I which presents the grid refinement analysis. To reduce the computation time, uniform but different grids are used in the axial direction. A fine grid near the channel entrance is used to capture the steep changes in the local Nusselt number while coarse grids are used in the downstream.

Discussion of results

The effect of several parameters such as Darcy number, microscopic inertial coefficient, and porous substrate thickness are presented in this section. The results show the effects of these parameters on the hydrodynamic field and thermal field. The numerical computations are verified by plotting Figure 2, which shows acceptable matching between the present fully developed axial velocity profile and the analytical Poiseuille parabola (White, 1991). This Figure proves the adequacy of the used finite difference schemes, since it was produced for $Da \rightarrow \infty$ and $A \rightarrow 0$. Another verification of the results is the matching of the computed fully developed Nusselt number, found to be 7.54, with previous work (Bejan, 1984).

The present results and graphs were obtained for the following typical conditions:

$$Pr_1 = 0.72, k_R = 1, \mu_R = 1, \rho_R = 1, C_R = 1, U_o = 100.$$

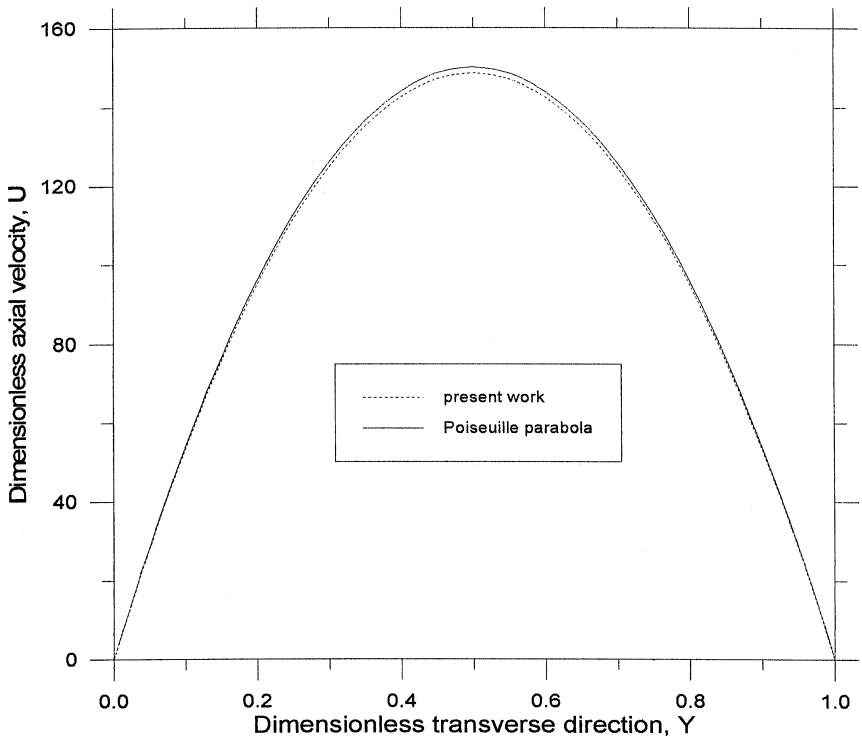

Figure 2.
Comparison of present fully developed axial velocity profile, U, with the analytical solution of the Poiseuille flow, for Da = 1.E+30, A= 1.E–30 and e = 0.4

Figure 3 shows that as Darcy number increases, the axial velocity, U, increases in the porous substrate, and due to continuity, the axial velocity decreases in the clear region. It is clear that as Darcy number decreases the porous substrate becomes dense and less permeable to fluid flow such that the fluid is forced to escape to the clear region. Therefore, the maximum axial velocity in the clear region increases and shifts towards the wall causing a reduction in the boundary layer thickness and an increase in the macroscopic shear force. Figure 4 shows that as the microscopic inertial coefficient decreases, the substrates become permeable for the fluid and as a result the axial velocity, U, increases in the porous substrate. Increasing the microscopic inertial term, by increasing A, and increasing the microscopic viscous term, by decreasing Da, have the same effect of increasing the retardation force which resists the fluid flow. The effect of the porous substrate thickness on the axial velocity profile is shown in Figure 5. It is clear that increasing porous layer thickness forces more fluid to escape to the clear region. Also, it is clear that the velocity distribution in the porous substrate is almost a uniform slug pattern except near the boundary at which the flow satisfies the no-slip boundary condition. Also, an important non-monotonic trend appears between maximum velocity and thickness. It appears that as porous substrate thickness increases the maximum velocity and velocity gradient at the wall increase but after optimum

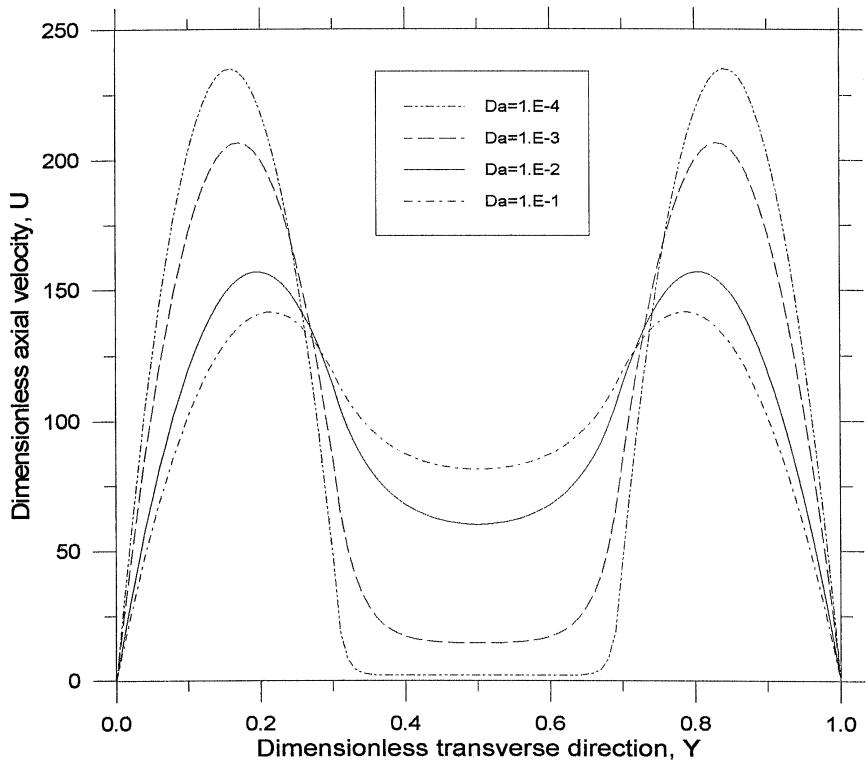

Figure 3.
Effect of Darcy number on the axial velocity profile, U, at X = 30, for A = 1, and e = 0.4

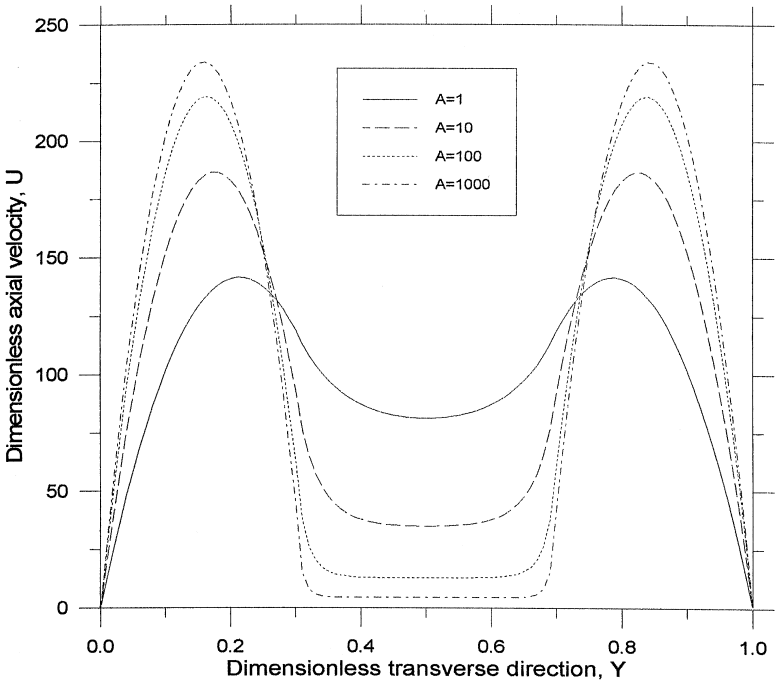

Figure 4.
Effect of form drag coefficient on the axial velocity profile, U, at X = 30, for Da = 0.1 and e = 0.4

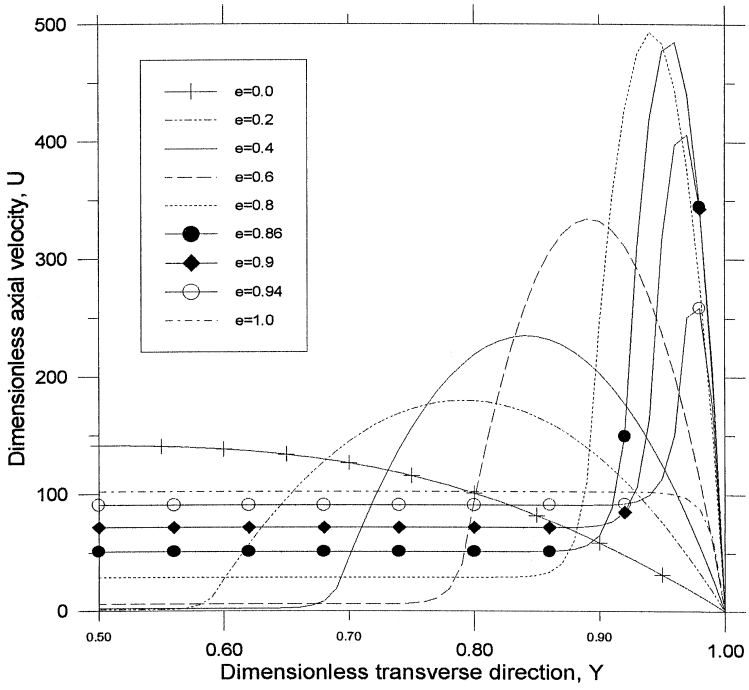

Figure 5.
Effect of porous substrate thickness on the axial velocity profile, U, for Da = 1.E–4 and A = 1, at X = 3

thickness this trend is reversed and the maximum velocity and its gradient at the wall decrease. The explanation of this trend is that for thin porous substrate thickness the microscopic drag forces dominate over macroscopic ones and force fluid to escape to the clear region. While for thick porous substrate, the macroscopic drag force is dominant and, therefore, it forces the fluid to escape to the porous region. The developing velocity profile is traced in the axial direction in Figure 6. It is noticed that, due to microscopic forces, the magnitude of the axial velocity is relatively low in the porous substrate especially at fully developed region. The magnitude of the axial velocity, U, decreases on marching along the channel. The flow retarded from the porous substrate, enhances the flow in the clear region, and as a result the velocity increases in the clear region. It is obvious from Figures 7 and 8 that as the thickness of the porous substrate decreases, both shear and inertial microscopic drag forces decrease, and as a result, the pressure drop reduces. The microscopic shear and inertial drag terms in the momentum equation have a negative sign and they resemble a retarding forces for the fluid flow. Also, these figure show that as Darcy number decreases or microscopic inertial coefficient increases the porous substrate becomes denser. Therefore, both shear and inertial microscopic drag forces increase and cause more pressure drop.

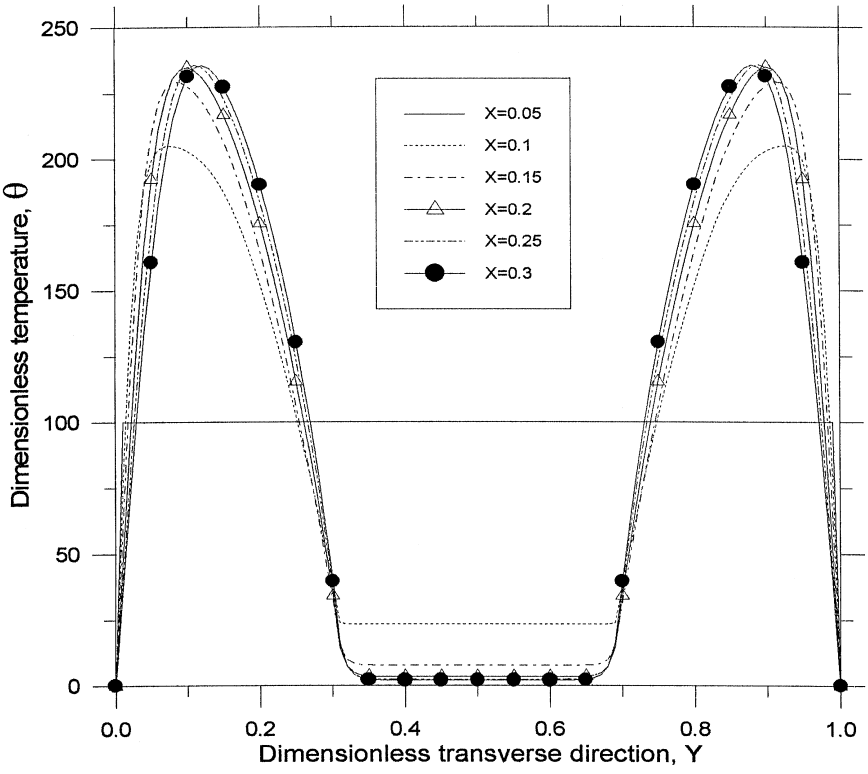

Figure 6.
Axial velocity profile as marching in the developing region, for Da = 1.E–4, A = 1, and e = 0.4

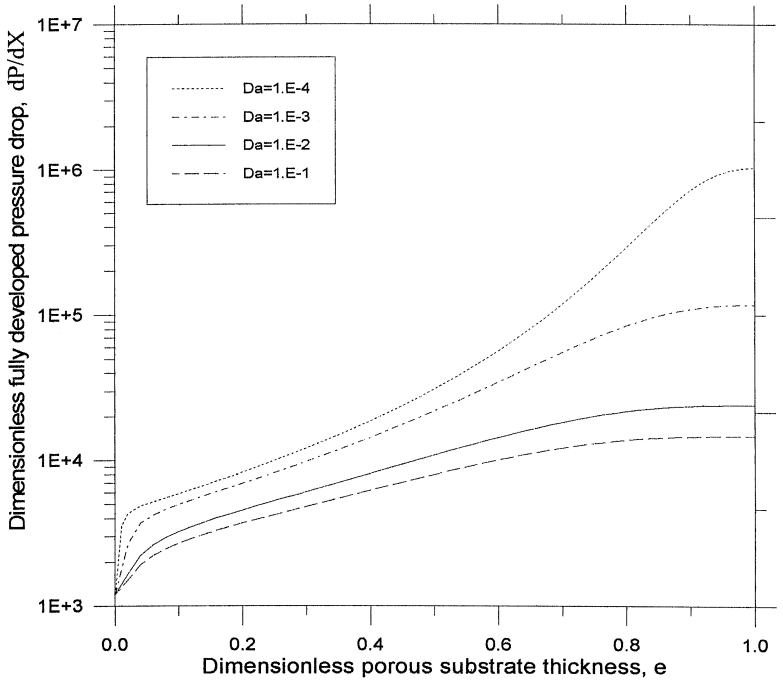

Figure 7.
Dimensionless fully developed pressure drop vs the porous substrate thickness for Kr = 1 and A = 1

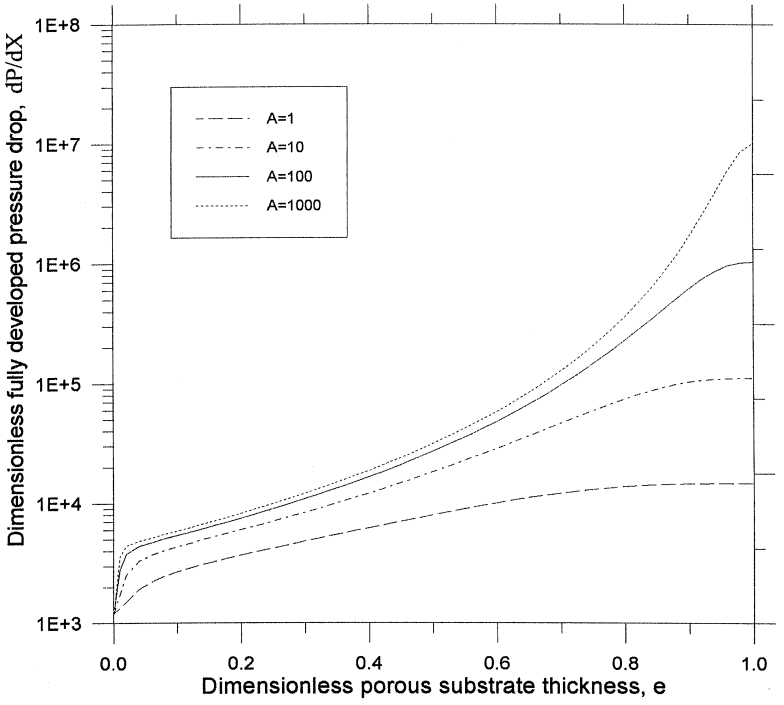

Figure 8.
Dimensionless fully developed pressure drop vs the porous substrate thickness for Kr = 1 and A = 1

It is expected to observe a strong effect of porous substrate on the thermal field, since the porous substrate has greatly affected the velocity field. Figures 9 and 10 show the effect of porous insertion on temperature profile. It is clear that as Darcy number increases or microscopic inertial coefficient decreases the porous substrate behaves as a solid substrate with a uniform temperature. This is explained by the small magnitude of pore velocity. Therefore, as Darcy number decreases or microscopic inertial coefficient increases the mixing cup temperature increases, which mean higher Nusselt number and better heat transfer. In Figure 11, it is observed that that Nusselt number decreases along the channel. This reduction in Nusselt number is due to the increase in the boundary layer thickness. The most important results of this study are Figures 12 and 13, since they show that it is possible to increase Nusselt number by a factor of four or even higher by using porous substrate. The figures show non-monotonic trend between Nusselt number and thickness. Also, they prove that partially filled duct has better performance than fully filled duct since it shows higher Nusselt number and at the same time less pressure drop. The non-monotonic behavior of Nusselt number is due to non-monotonic trend of velocity with thickness that has affected the temperature profile resulting in non-monotonic effect of temperature with thickness. This temperature trend will cause non-monotonic trend of mixing cup temperature with thickness. Based on Nusselt number definition, $Nu \sim (dT/dY)_{y=0}/(T_w - T_m)$,

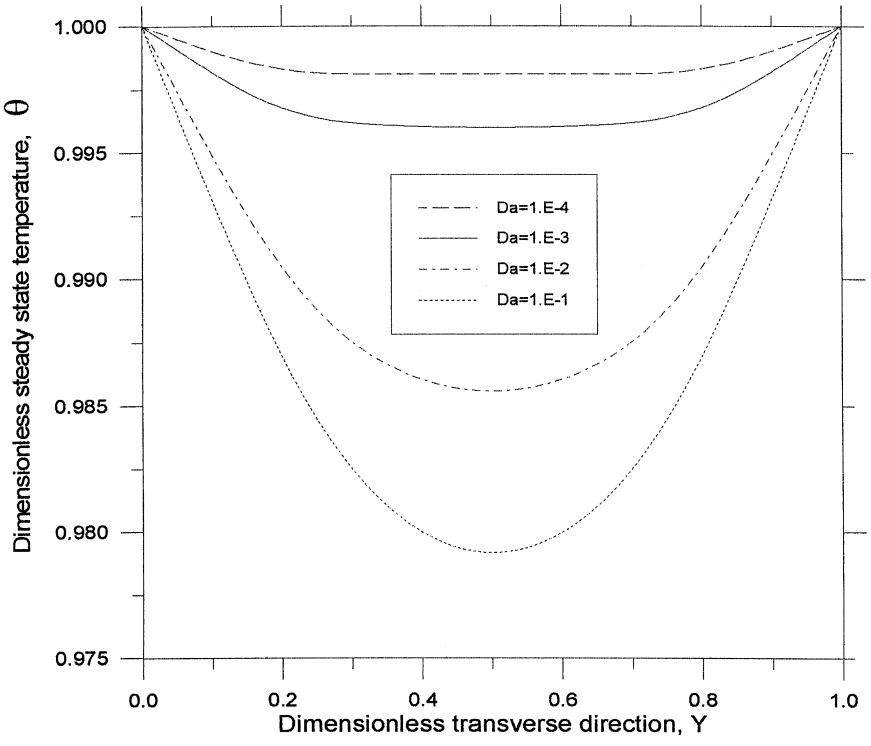

Figure 9.
Effect of Darcy number on the temperature profile, U, at X = 2, for A = 1, Kr = 1, and e = 0.4

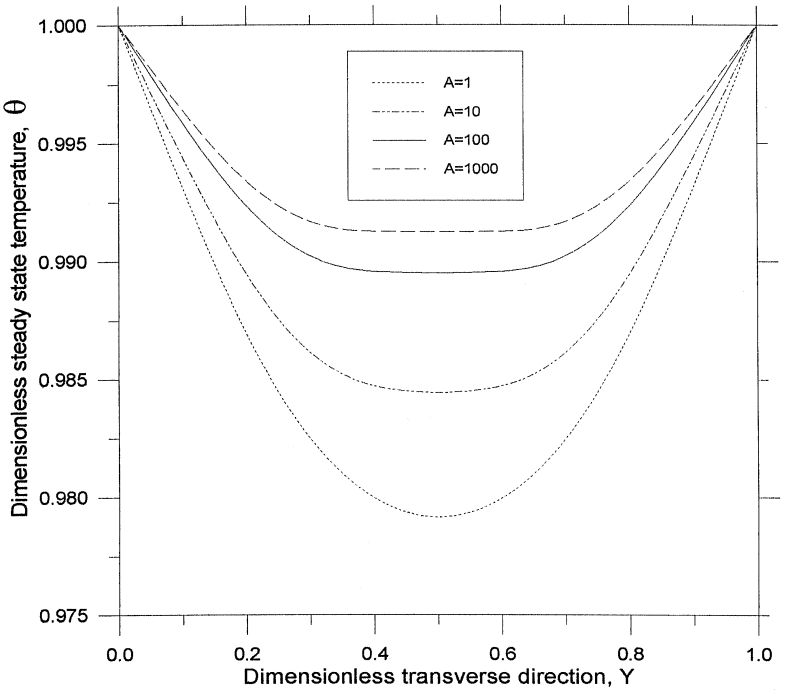

Figure 10.
Effect of form drag coefficient on the temperature profile at X = 2, for Da = 0.1, Kr = 1, and e = 0.4

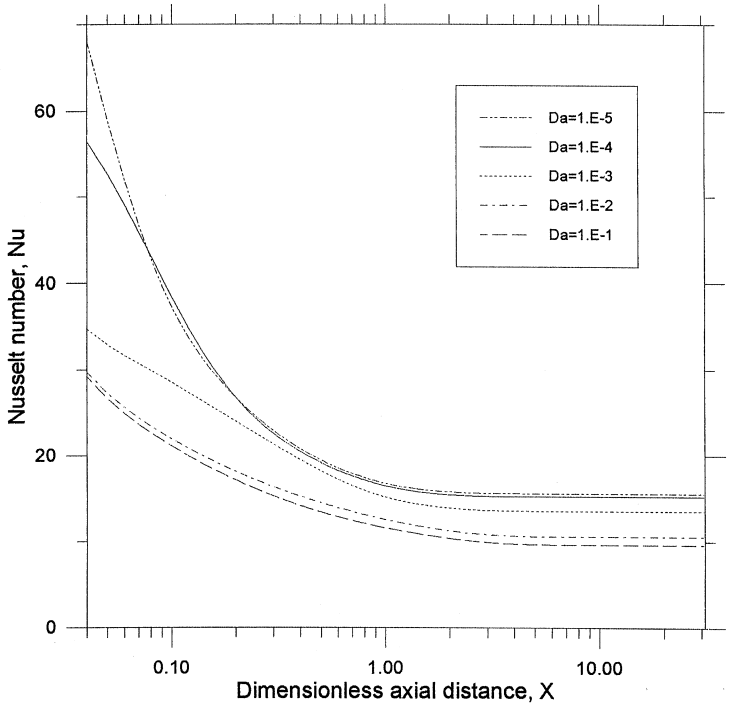

Figure 11.
Nusselt number vs dimensionless axial direction, X, for different porous substrate thicknesses, for A = 1, Kr = 1, and e = 0.4

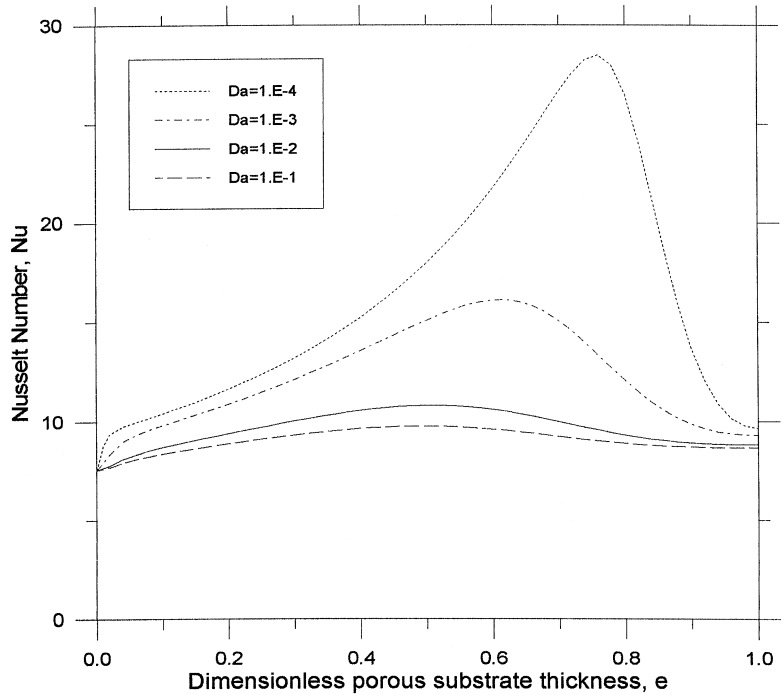

Figure 12.
Fully developed Nusselt number vs porous substrate thickness, for A = 1 and Kr = 1

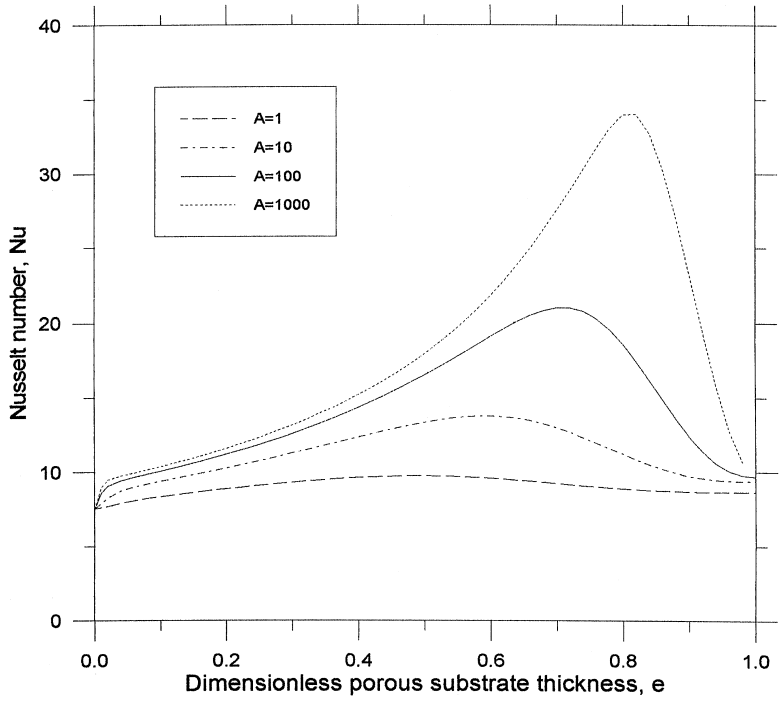

Figure 13.
Fully developed Nusselt number vs porous substrate thickness, for A = 1 and Kr = 1

it is obvious and due to non-monotonic trend of temperature profile that Nusselt number will have similar trend. Figures 12 and 13 show that for porous substrate thickness equal to zero, the value of Nusselt number approaches the constant value 7.54, which presents the Nusselt of a clear isothermal parallel wall duct as reported by Bejan (1984). As was previously mentioned, Darcy number has inverse trend with microscopic inertial coefficient, A, this is notified from Figures 12 and 13. As Darcy number decreases or as microscopic inertial coefficient increases the value of Nusselt number approaches similar value of clear duct.

Conclusions

A numerical solution is adopted to simulate the problem of transient developing forced convection flow between two isothermal parallel-plates channel partially filled with porous substrate. The Brinkman-Forchheimer-extended Darcy model was used to model the flow inside the porous domain. The present study reports the effects of porous layer thickness, Darcy number, and microscopic inertial coefficient on the thermal performance of the system under consideration. It is found that there is non-monotonic relation between Nusselt number and the thickness of the porous substrate.

Porous media enhance forced convection heat transfer by reducing the boundary layer thickness or by using high thermal conductive material, since higher thermal conductivity allows more heat flow to be conducted to the fluid. Small Darcy numbers or large values of microscopic inertial coefficient reduce hydrodynamic boundary layer thickness. The effect of Darcy number and microscopic inertial coefficient in the developing region is higher than that in the fully developed region, because as one progresses through the channel the magnitude of the pore velocity in the porous domain decreases.

Increasing porous substrate up to optimum thickness improves Nusselt number while beyond this optimum thickness any increment of porous substrate thickness will reduce Nusselt number. Generally, forced convection can be significantly enhanced by using porous substrate insertion, provided that high effective thermal conductivity and dense porous substrate is used.

References

Al-Nimr, M.A. and Alkam, M. (1997), "Unsteady non-Darcian forced convection analysis in an annuls partially filled with a porous material", *J. of Heat Transfer*, Vol. 119, pp. 1-6.

Al-Nimr, M.A. and Alkam, M. (1998), "Unsteady non-Darcian fluid flow in parallel channels partially filled with porous materials", *Heat and Mass Transfer*, Vol. 33, pp. 315-18.

Alkam, M. and Al-Nimr, M.A. (1998), "Transient-non-Darcian forced convection flow in a pipe partially filled with a porous material", *Int. J. Heat and Mass Transfer*, Vol. 41, pp. 347-56.

Alkam, M. and Al-Nimr, M.A. (1999a), "Solar collectors with tubes partially filled with porous substrate", *J. of Solar Energy Engineering*, Vol. 121, pp. 20-4.

Alkam, M. and Al-Nimr, M.A. (1999b), "Improving the performance of double-pipe heat exchanger by using porous substrates", Accepted for publication in *Int. J. Heat and Mass Transfer*.

Alkam, M., Al-Nimr, M.A. and Mousa, N.Z. (1998), "Transient forced convection of non-Newtonian fluid in the entrance region of porous concentric annuli", *Int. Numerical Methods for Heat and Fluid Flow*, Vol. 8 No. 5, pp. 703-16.

Beavers, G.S. and Joseph, D.D. (1967), "Boundary conditions at naturally permeable wall", *J. Fluid Mech.*, Vol. 13, pp. 197-207.

Bejan, A. (1984), *Convection Heat Transfer*, John Wily and Sons, New York, NY.

Bodoia, J.R. and Osterle, J.F. (1961), "Finite-difference analysis of plane Poisseuille and Couette flow developments", *Applied Science Research*, Vol. A10, pp. 265-76.

Carman, P.C. (1956), *Flow of Gases Through Porous Material*, Academic Press, New York, NY.

Chen, S.C. and Vafai, K. (1996), "Analysis of free surface momentum and energy transport in porous media", *Numerical Heat Transfer A*, Vol. 30, pp. 281-96.

Chikh, S., Boumedien, A., Bouhadef, K. and Lauriat, G. (1995a), "Analytical solution of non-Darcian forced convection in an annular duct partially filled with a porous medium", *Int. J. Heat and Mass Transfer*, Vol. 38, pp. 1543-51.

Chikh, S., Boumedien, A., Bouhadef, K. and Lauriat, G. (1995b), "Non-Darcian forced convection analysis in an annular partially filled with a porous material", *Numerical Heat Transfer A*, Vol. 28, pp. 707-22.

Collins, R.E. (1961), *Flow of Fluids Through Porous Material*, Reinhold, New York, NY.

El-Shaarawi, M.A. and Alkam, M.K. (1992), "Transient forced convection in the entrance region of concentric annuli", *Int. J. Heat and Mass Transfer*, Vol. 35, pp. 3335-44.

Hoffman, J.D. (1992), *Numerical Method for Engineering and Scientists*, Purdo University.

Jang, J.Y. and Chen, J.L. (1992), "Forced convection in a parallel plate channel partially filled with a high porosity medium", *Int. Comm. Heat Mass Transfer*, Vol. 19, pp. 263-73.

Jiang, P.X., Wang, B.X., Luo, D.A. and Ren, Z.P. (1996), "Fluid flow and convection heat transfer in a vertical porous annulus", *Numerical Heat Transfer A*, Vol. 30, pp. 305-20.

Kaviany, M. (1995), *Principle of Heat Transfer in Porous Media*, 2nd ed., Spring, New York, NY.

Nield, D.A. (1991), "The limitation of the Brinkman-Forchheimer equation in modeling flow in a saturated porous medium and at an interface", *Int. J. Heat and Fluid Flow*, Vol. 12, pp. 269-72.

Poulikakos, D. and Kazmierczak, M. (1987), "Forced convection in a duct partially filled with a porous material", *J. of Heat Transfer*, Vol. 109, pp. 653-62.

Poulikakos, D. and Renken, K. (1987), "Forced convection in a channel filled with a porous medium, including the effect of flow inertia, variable porosity, and Brinkman friction", *J. of Heat Transfer*, Vol. 109, pp. 880-8.

Rudraiah, N. (1985), "Forced convection in a parallel plate channel partially filled with a porous material", *J. of Heat Transfer*, Vol. 107, pp. 332-1.

Vafai, K. and Kim, S.J. (1990), "Fluid mechanics of interface region between a porous medium and fluid layer – an exact solution", *Int. J. Heat and Fluid Flow*, Vol. 11, pp. 254-6.

Vafai, K. and Kim, S.J. (1995), "On the limitations of the Brinkman-Forchheimer-extended Darcy equation", *Int. J. Heat and Fluid Flow*, Vol. 16, pp. 11-15.

Vafai, K. and Thiyagaraja, R. (1987), "Analysis of flow and heat transfer at the interface region of a porous medium", *Int. J. Heat and Mass Transfer*, Vol. 30, pp. 1391-405.

White, F.M. (1991), *Viscous Fluid Flow*, McGraw-Hill, Maidenhead, ISBN 0-07-100995-7.